2016 IEEE 55th Conference on Decision and Control (CDC)
ARIA Resort & Casino
December 12-14, 2016, Las Vegas, USA

Range Based Control Law to Generate Patterns With a Unicycle

Twinkle Tripathy, Arpita Sinha, Hemendra Arya and Aseem Borkar

***Abstract*— The paper focuses on generating patterns in a plane that can serve several applications like (irregular-boundary) coverage, (differentiated) surveillance, etc. These patterns are centred around a stationary point, termed as target. For practical purposes, a target point can be any landmark, beacon, etc. A control law is proposed as a continuous function of range information (distance between the agent and target) to generate a periodic annular pattern under certain conditions. Also, a switching strategy is presented to switch the agent trajectory periodically among these annular patterns. Simulation and experimental results have been presented to validate the theoretical results.**

I. INTRODUCTION

The spirals in a sunflower, the trajectories of dragon-flies in flight, the hypotrochoidal paths of astronomical objects are a few examples of the vast diversified types of patterns occurring in the nature. These patterns have attracted the researchers in the control and robotics community for several decades now. The generation of these aesthetically patterns either help in better understanding of kinematics of systems or serve civilian purposes like surveillance, coverage [2], etc.

The literature available in the area of control and robotics present several control/guidance schemes that reproduce some of the naturally existing patterns by using either single/multiple autonomous agents. The generation of patterns can be achieved broadly by two ways: (a) spacial arrangements of multiple agents (b) trajectories of single/multiple agents. The patterns generating out of the spacial arrangements of multiple agents (by introducing local/global interaction among the agents) fall into the category of formation control [1]. Patterns generated by shaping the trajectories of the agents([4]-[8]), which is more relevant for the current work, can be achieved by single or multiple agents with/without inter-agent communication. A commonly used method for shaping the trajectory is through trajectory tracking strategies [3]. However, this can also be achieved without defining a reference trajectory ([2],[4]-[12]). In [4], Juang proposes to use the generalised cyclic pursuit strategy for the generation of epicyclic motions for multiple agents modeled with single integrator kinematics. The paper augments the standard pursuit control with a rotation and stabilisation term for each of the agents. In [5]-[6], Galloway *et al.* examine a constant bearing based pursuit strategy to establish the existence of a family of rectilinear relative equilibria that results in periodic orbit for multiple autonomous agents. Tsiotras *et al.* propose a standard feedback in [7]-[8] for multi-agent consensus problems by the addition of the control law with a term perpendicular to the relative distance between two agents. The resulting control law renders flexibility with respect to the achievable patterns.

Twinkle Tripathy, Arpita Sinha and Aseem Borkar are with Systems and Control Engineering Group at IIT Bombay, India, Hemendra Arya is with Aerospace Engineering Department, IIT Bombay, India, twinkle.tripathy@sc.iitb.ac.in, arpita.sinha@iitb.ac.in, arya@aero.iitb.ac.in and aseem@sc.iitb.ac.in.

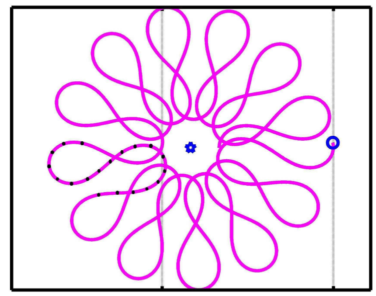

Fig. 1: Annular pattern

The current work focuses on generating patterns in a plane bound within an annulus with a single autonomous agent, which is modeled with unicycle kinematics. For the proposed control law, the patterns are usually centred about a stationary point called the target point (which could represent any landmark, beacon, etc. depending on the application). Now, the control is designed using only range information where range refers to the distance between the agent and the target. A preliminary analysis for the generation of hypotrochoid-like patterns, has been presented in [9]-[12] for which the control law is a linear or specific non-linear function of range. For this work, the paper proposes to use any continuous function of range as input and establishes conditions for the generation of bounded periodic patterns (always bound within an annulus) as shown in Fig. 1. Further, the paper presents a switching strategy which results in a wide variety of patterns formed by the alternate switching of the agent trajectory between any two annular patterns. The theoretical results have been validated by simulation and experiments performed using a single Firebird V robot.

The paper is organised in the following manner: Section II illustrates the problem being considered in the current work and gives conditions for the generation of bounded patterns. Section III presents the switching strategy and requirements under which switching of the trajectory between any two patterns is feasible. These results have been validated in simulation in Section IV. Description of experimental results, performed to validate the same, have been given in Section V. Finally, Section VI concludes the paper and suggests

978-1-5090-1837-6/16/$31.00 ©2016 IEEE

possible future work.

II. Problem description

The paper focusses on the generation of myriad shapes and patterns on a plane by using a single autonomous agent. The autonomous agent is modeled as a unicycle whose kinematics is given by,

$$\begin{aligned}\dot{x}(t) &= v\cos\alpha(t)\\ \dot{y}(t) &= v\cos\alpha(t)\\ \dot{\alpha}(t) &= u(t),\end{aligned} \tag{1}$$

where $(x(t), y(t))$ and $\alpha(t)$ denote the position coordinates and heading angle of the agent at any time t. The inputs to the agent can be linear speed v and angular speed $\dot{\alpha}(t)$. Here, v is assumed to be a positive constant and, hence, the control input to the agent is the angular speed denoted by $u(t)$. The framework of the paper consists of the autonomous agent, a stationary target (denoted by (x_T, y_T)) and the availability of only distance information to the agent. For this work, the agent uses the distance information between the target and itself, termed as range r. Considering that only range information is available, the control input is designed as,

$$u = f(r) \tag{2}$$

where $f(r)$ is any continuous real valued function of r. Substituting (2) in kinematics (1), we get $\dot{\alpha} = f(r)$. Using this, the kinematics of the agent can be transformed into polar coordinates as,

$$\dot{r} = -v\cos(\alpha-\theta) \tag{3}$$

$$\dot{\theta} = -v\cos(\alpha-\theta) \tag{4}$$

$$\dot{\alpha} = f(r) \tag{5}$$

where, in reference to Fig. 2, θ denotes the line-of-sight(LOS) angle between the agent and the target. Interestingly, the system of equations in (3)-(5) can be simplified and reduced into a system of two variables. For the same, a variable $\phi = \alpha - \theta$ is introduced and substituted in eqns. (3)-(5). So, ϕ represents the angle between the velocity vector of the agent and its line-of-sight with the target. The simplified kinematics is given by,

$$\dot{r} = -v\cos\phi \tag{6}$$

$$r\dot{\phi} = rf(r) + v\sin\phi. \tag{7}$$

Eqns. (6)-(7) give the relationship between the variables r and ϕ from which $dr/d\phi$ is computed and then rearranged to get,

$$(rf(r) + v\sin\phi)dr + vr\cos\phi \; d\phi = 0. \tag{8}$$

Depending on $f(r)$, the differential equation (8) could be either exact or non-exact. For the latter, an integrating factor could be used to make (8) exact [13]. For both the cases, the solution of (8) is always given by,

$$\tilde{f}(r) + vr\sin\phi = K \tag{9}$$

where $\tilde{f}(r) \in \mathbb{C}^1$ does not have any constant term and satisfies the condition $f(r) = \frac{1}{r}\frac{d}{dr}\tilde{f}(r)$. Further, K can be calculated from the initial conditions, $r_0 (= r(0))$ and $\phi_0 (= \phi(0))$ as,

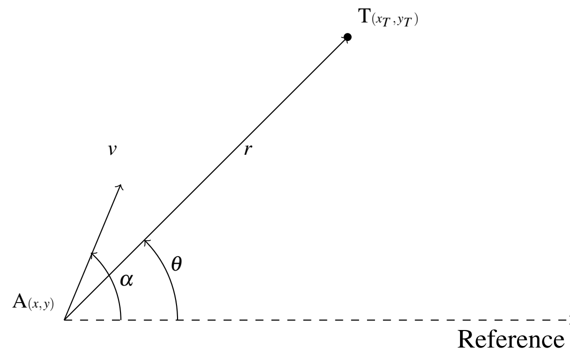

Fig. 2: Planar geometry between the agent and the target point

$$K = \tilde{f}(r_0) + vr_0\sin\phi_0. \tag{10}$$

On re-arranging (9), we get,

$$g(r) = -vr\sin\phi \tag{11}$$

where $g(r)$ is termed as the generating function for $f(r)$, such that,

$$g(r) = \tilde{f}(r) - K \tag{12}$$

$$f(r) = \frac{1}{r}\frac{d}{dr}g(r). \tag{13}$$

For any $f(r)$, the generating function $g(r) \in \mathbb{C}^1$ and varies with K. Given $f(r)$ and K, any solution of (11) is an intersection of $g(r)$ with straight $(v\sin\phi)r$ for different values of ϕ. Now $\sin\phi \in [-1, 1]$, hence, any point on $g(r)$ satisfies (11) only when $-vr \le g(r) \le vr$. Thus, region between straight lines $\pm vr$, shaded in gray in Fig. 3, denotes the possible region in which the behaviour of $g(r)$ is studied; the solution set of (11) is given by $\left(r, \sin^{-1}\left(-\frac{g(r)}{vr}\right)\right)$ such that $-vr \le g(r) \le vr$. Now, we are interested in finding the conditions on the generating function $g(r)$ such that the unicycle generates annular patterns in a plane.

Lemma 1: The trajectory of an autonomous agent, with kinematics (3)-(5), is a periodic and annular pattern, bounded by inner radius $R_{\min}$ and outer radius $R_{\max}$, if any generating function $g(r) \in \mathbb{C}^1$ satisfies the following,

(a) $-vr < g(r) < vr$ for all $r \in (R_{\min}, R_{\max})$,
(b) $g(R_{\min}) = \pm vR_{\min}$,
(c) $g(R_{\max}) = \pm vR_{\max}$,
(d) $\frac{d}{dr}g(r)|_{r\in\{R_{\min},R_{\max}\}} \notin \{-v, v\}$.

Then, the control input and initial conditions (r_0, ϕ_0) are given by,

(e) $f(r) = \frac{d}{dr}g(r)$
(f) $r_0 \in [R_{\min}, R_{\max}]$ and ϕ_0 is given by (11).

Proof: For any ϕ, $\sin\phi \in [-1, 1]$. Then, at any instantaneous r, (12) implies,

$$-vr \le g(r) \le vr. \tag{14}$$

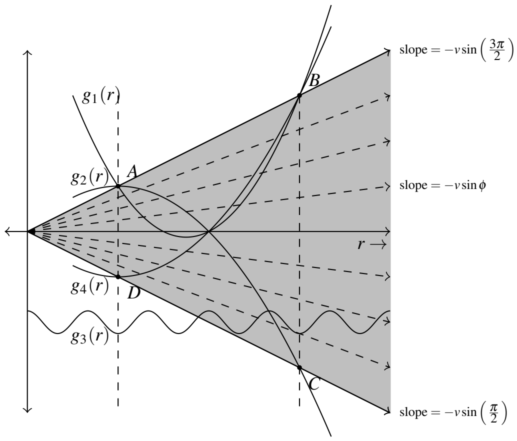

Fig. 3: Generating functions $g(r)$s

Now, for an annular pattern, instantaneous r must lie in $[R_{\min}, R_{\max}]$. Then, (14) must hold for all $r \in [R_{\min}, R_{\max}]$. At any extrema of r, $\dot{r} = 0$. Then, (6) implies $\phi \in \{\frac{\pi}{2}, \frac{3\pi}{2}\}$. Since $R_{\min}$ and $R_{\max}$ are extrema of r, substituting the values of ϕ in (11), we get conditions (b) and (c).

Suppose $\phi|_{r=\bar{r}} \in \{\frac{\pi}{2}, \frac{3\pi}{2}\}$ at any $\bar{r} \in (R_{\min}, R_{\max})$. Then, using (11), $g(\bar{r}) = \pm v\bar{r}$ and $\dot{r} = 0$. Let $\phi|_{r=\bar{r}} = \frac{3\pi}{2}$, then $g(\bar{r}) = v\bar{r}$. If $\frac{d}{dr}g(\bar{r}) \neq v$, then it can be easily shown that there exists $r \in [R_{\min}, R_{\max}]$ where (14) is violated. Again, if $\frac{d}{dr}g(r) = v$, then using (13), $f(\bar{r}) = \frac{1}{r}\frac{d}{dr}g(r) = \frac{v}{\bar{r}}$. Then, all the other higher derivatives of r and ϕ are nullified. Similar arguments hold when $\phi|_{r=\bar{r}} = \frac{\pi}{2}$. Thus, if $r(t_1) = \bar{r}$ at time $t_1 > 0$, then $r(t) = \bar{r}$ for all time $t \geq t_1$. However, $\dot{\alpha} = f(\bar{r}) = \pm\frac{v}{\bar{r}}$ and $\dot{\theta} = -\frac{v\sin\phi_{\bar{r}}}{\bar{r}} \neq 0$ become constant. Hence, the unicycle starts moving in a circular trajectory with radius $\bar{r}$. Thus, in order to get an annular trajectory, conditions (a) and (d) are mandatory for all $r \in (R_{\min}, R_{\max})$. Further, condition (a) ensures $\phi \neq \{\pi/2, 3\pi/2\}$ which implies $\dot{r} \neq 0$. Hence, there are no local extrema and r increases monotonically from $R_{\min}$ to $R_{\max}$ and decreases monotonically from $R_{\max}$ to $R_{\min}$.

Let us assume that at time $t = t_1$, the agent trajectory is at $(R_{\min}, \bar{\phi}_1)$ where $\bar{\phi}_1 \in \{\frac{\pi}{2}, \frac{3\pi}{2}\}$. Then, using (10), $K = \tilde{f}(R_{\min}) + vR_{\max}\sin\bar{\phi}_1$. As explained before, $r(t)$ increases to $R_{\max}$ from $r = R_{\min}$. Then, at time $t = t_1 + T$, $r(t)$ decreases again to $R_{\min}$ and ϕ becomes $\bar{\phi}_2$. $K = \tilde{f}(R_{\max}) + vR_{\max}\sin\bar{\phi}_1 = \tilde{f}(R_{\max}) + vR_{\max}\sin\bar{\phi}_3$, from (10). Hence, $\bar{\phi}_1 = \bar{\phi}_2$ implying that the agent achieves the same state $(R_{\min}, \bar{\phi}_1)$ after T units of time. Since the agent follows the same kinematics (1) from there, it keeps reaching $(R_{\min}, \phi_1)$ in fixed intervals, resulting in a periodic annular trajectory.

Once a suitable generating function is obtained, the control input can be found by using condition (e). Condition (f) ensures that (r_0, ϕ_0) is a point on the pattern. Thus, proved. ■

Lemma 1 gives the necessary conditions on generating function $g(r)$, hence, $f(r)$ to generate an annular and periodic pattern. For example, for $R_{\max} = 6$ and $R_{\min} = 2$, $f(r)$ for the generating functions $g_1(r) = 0.5r^2 - 3.5r + 6$, $g_2(r) = 0.25r^2 - r$ and $g_3(r) = -0.25r^2 + r$, shown in Fig. 3, result in annular trajectories as they satisfy Lemma 1. However, $f(r)$ for $g_3(r) = -2 + 0.25\cos(1.5\pi r)$ does not result in an annular pattern.

As explained before, annular patterns can serve several applications like surveillance, coverage and so on. However, for applications like irregular-boundary coverage, differentiated surveillance (in which that the surveillance is stricter for areas with higher priority), etc. annular patterns may not be very suitable. To address this problem, we propose a switching strategy which results in wider set of patterns as shown in Figs. 4 and 5 in which agent trajectory intermittently and periodically switches between different patterns.

III. Switching between patterns

In this section, we explore ways to generate patterns which are beyond the annular and periodic patterns explored in Section II by making agent trajectory switch between different patterns periodically as shown in Fig. 4. Next, we present the necessary conditions to achieve a switching trajectory. These results can be easily extended to achieve switching between any number of patterns.

A. Direct Switching Strategy

Here, we propose a switching strategy which enables the agent trajectory to switch directly(without any transient or intermediate trajectory) between two patterns periodically with time. For the same, we introduce a term cycle defined as follows:

Definition 1: Starting at any (r^*, ϕ^*), the path traversed by the agent till it reaches the state (r^*, ϕ^*) again is defined as cycle.

In a cycle, owing to the periodicity of r, any $r^* \notin \{R_{\min}, R_{\max}\}$ occurs twice and $r^* \in \{R_{\min}, R_{\max}\}$ occurs once. Graphically, a cycle is explained as the dotted path of the curve shown in Fig. 1. While switching between the patterns, by varying the number of cycles of each pattern after which switching occurs, a variety of switching trajectories can be generated for the same two specified patterns. The subsequent Lemma gives the conditions to switch between two different patterns directly.

Lemma 2: Consider generating functions $g_1(r)$ and $g_2(r)$ that generate annular patterns with inner radii $R_{\min 1}$, $R_{\min 2}$ and outer radii $R_{\max 1}$, $R_{\max 2}$, respectively. Then, the agent trajectory switches between the patterns by using control input,

$$u = \begin{cases} \frac{1}{r}\frac{d}{dr}g_1(r) & r = \bar{r}, \frac{n}{mk_1} \in \mathbb{N} \text{ and is even} \\ \frac{1}{r}\frac{d}{dr}g_2(r) & r = \bar{r}, \frac{n}{mk_2} \in \mathbb{N} \text{ and is odd} \end{cases} \tag{15}$$

only when there exists $\bar{r} \in [R_{\min 1}, R_{\max 1}] \cap [R_{\min 2}, R_{\max 2}]$ such that

$$g_1(\bar{r}) = g_2(\bar{r}), \tag{16}$$

where $n \in \mathbb{N}$, $m \in \mathbb{N}$ and $k_{j \in \{1,2\}} = \begin{cases} 1 & \bar{r} \in \{R_{\min j}, R_{\max j}\} \\ 2 & \bar{r} \in (R_{\min j}, R_{\max j}) \end{cases}$ denote the number of times instantaneous r reaches $\bar{r}$, the desired number of cycles after which the trajectory switches between the patterns and the number of times $\bar{r}$ occurs in a cycle, respectively.

Proof: Suppose $\bar{r}$ is a point at which the agent can switch between the two specified trajectories. Then, $g_2(\bar{r}) = g_1(\bar{r})$ at $\bar{r}$ and $\bar{\phi} = \phi \mid_{r=\bar{r}}$ can be calculated using (11) for either $g_1(r)$ or $g_2(r)$. Then, $\bar{r}$ is the intersection of $g_1(r)$ and $g_2(r)$. Further, it ensures that $(\bar{r}, \bar{\phi})$ is a point on both the patterns. Since θ is common for both patterns at the point of switching $(\bar{x}, \bar{y})$, the instantaneous α also is the same to achieve $\phi = \bar{\phi}$. This ensures the continuity of α while switching.

Using Lemma 1, since $(\bar{r}, \bar{\phi})$ satisfy (11) for both $g_1(r)$ and $g_2(r)$, $\bar{r}$ must belong to $[R_{\min 1}, R_{\max 1}] \cap [R_{\min 2}, R_{\max 2}]$. If not, then $(\bar{r}, \bar{\phi})$ violates (11) for either $g_1(r)$ or $g_2(r)$. Then, trajectory can not be switched directly between the two specified patterns.

Fir $j \in \{1,2\}$, consider any $g_j(r)$, under the corresponding control law given by (12), the agent generates the desired annular and periodic pattern. r varies periodically between $R_{\max j}$ and $R_{\min j}$, incrementing n each time r reaches $\bar{r}$. $\bar{r}$ occurs mk_j times for m number of cycles. When $\frac{n}{mk_j} \in \mathbb{N}$, the trajectory completes the desired number of cycles of the pattern. Since, the $(\bar{r}, \bar{\phi})$ is a point on both the patterns, by using the control input given in (15), the agent starts tracing the other pattern. Similarly, r keeps varying between its maximum and minimum until $\frac{n}{mk_j} \in \mathbb{N}$, then trajectory switches to the other pattern. Thus, proved. ■

Lemma 2 shows that direct switching can occur between two patterns only at the intersection points of their generating functions. However, Lemma 2 can not be used if,

(a) $[R_{\min 1}, R_{\max 1}] \cap [R_{\min 2}, R_{\max 2}] = \emptyset$
(b) there does not exist $\bar{r} \in [R_{\min 1}, R_{\max 1}] \cap [R_{\min 2}, R_{\max 2}]$ such that $g_1(\bar{r}) = g_2(\bar{r})$
(c) agent trajectory is required to be switched at points (say two points $\bar{r}_1$ and $\bar{r}$ with $\bar{r}_2 > \bar{r}_1$) more than the total intersection points.

To circumvent such situations, we propose to use an intermediate generating function. For example, for condition (c), an intermediate function $g_i(r) \in \mathbb{C}^1$ for all $r \in [\bar{r}_1, \bar{r}_2]$ is designed to transfer the trajectory from one pattern to another. The next subsection explains the same.

B. Intermediate-function based Switching Strategy

In situations where direct switching between two control inputs is infeasible, we propose to switch between patterns using an intermediate control input $f_i(r)$ $(f_1(r) \to f_i(r) \to f_2(r) \to f_i(r) \to f_1(r))$.

Theorem 1: Consider generating functions $g_1(r)$ and $g_2(r)$ that generate annular patterns with inner radii $R_{\min 1}$, $R_{\min 2}$ and outer radii $R_{\max 1}$, $R_{\max 2}$, respectively. Let any $\bar{r}_1 \in [R_{\min 1}, R_{\max 1}]$ and $\bar{r}_2 \in [R_{\min 2}, R_{\max 2}]$ be the points of switching. An intermediate generating function $g_i(r) \in \mathbb{C}^1$ is designed as,

(a) $g_i(\bar{r}_1) = g_1(\bar{r}_1)$
(b) $g_i(\bar{r}_2) = g_2(\bar{r}_2)$
(c) $-vr < g_i(r) < vr$ for all $r \in (\bar{r}_1, \bar{r}_2)$ assuming $\bar{r}_1 < \bar{r}_2$.

Then, the agent generates a switching pattern by using control inputs,

$$u = \begin{cases} \frac{1}{r}\frac{d}{dr}g_1(r) & \frac{n_1}{m_1 k_1} \notin \mathbb{N} \\ \frac{1}{r}\frac{d}{dr}g_i(r) & \begin{cases} r = \bar{r}_1 & \frac{n_1}{m_1 k_1} \in \mathbb{N} \\ r = \bar{r}_2 & \frac{n_2}{m_2 k_2} \in \mathbb{N} \end{cases} \\ \frac{1}{r}\frac{d}{dr}g_2(r) & \frac{n_2}{m_2 k_2} \notin \mathbb{N} \end{cases} \tag{17}$$

where $n_j \in \mathbb{N}$, $m_j \in \mathbb{N}$ and $k_j = \begin{cases} 1 & \bar{r} \in \{R_{\min}, R_{\max}\} \\ 2 & \bar{r} \in (R_{\min}, R_{\max}) \end{cases}$ denote the number of times instantaneous r reaches $\bar{r}_j$, the desired number of cycles of pattern corresponding to $g_j(r)$ and the number of times $\bar{r}_j$ occurs in a cycle, respectively for $j \in \{1,2\}$.

Proof: Here, we propose to switch between the patterns using an intermediate trajectory. The design of the corresponding intermediate generating function $g_i(r)$ is explained as follows: Without loss of generality, we choose any $\bar{r}_1 \in [R_{\min 1}, R_{\max 1}]$ and $\bar{r}_2 \in [R_{\min 2}, R_{\max 2}]$ such that $\bar{r}_1 < \bar{r}_2$. Now, $g_i(r)$ is designed such that $g_i(\bar{r}_1) = g_1(\bar{r}_1)$, $g_i(\bar{r}_2) = g_2(\bar{r}_2)$ and $g_i(r)$ satisfies Lemma 1 for any $R_{\min} < \bar{r}_1 < \bar{r}_2 < R_{\max}$. This ensures that following the control input corresponding to $g_i(r)$, the agent trajectory varies periodically between $(R_{\min}, R_{\max})$ and thus reaches both $\bar{r}_1$ and $\bar{r}_2$.

For $j \in \{1,2\}$, $\bar{r}_j$ occurs $m_j k_j$ times for m_j number of cycles, where k_j depends on the value of $\bar{r}_j$. Suppose agent starts with any g_1 (or $g_2(r)$), then it generates the corresponding pattern. Thereafter, as explained in the proof of Lemma 2, the agent trajectory switches to the intermediate pattern (corresponding to $g_i(r)$) when $n_1/(m_1 k_1)$ (or $n_2/(m_2 k_2)$) satisfies the conditions given in the Theorem. $g_i(r)$ takes the trajectory from the point $\bar{r}_1$ (or $\bar{r}_2$) to $\bar{r}_2$ (or $\bar{r}_1$). Then, the trajectory is again switched to the other pattern. Again, as n_2 (or n_1) satisfies the desired conditions, it switches back to the intermediate function. The intermediate trajectory switches to the first pattern as r reaches $\bar{r}_1$ (or $\bar{r}_1$). This keeps repeating to generate the periodic switching pattern. Thus, proved. ■

Theorem 1 guarantees that the agent trajectory can switch between any two annular patterns.

IV. Simulation Results

This section validates the results obtained in Sections II and III. For all the cases demonstrated here, we consider $v = 1$. Further, for each of the trajectories generating using switching strategy, different patterns in the trajectory have been shown in different colors.

Case 1 - *Annular pattern*: Given $R_{\min} = 1$ and $R_{\max} = 5$, we design a generating function $g(r) = \frac{r^3}{4} - \frac{9r^2}{8} - 1.875$. Hence, $g(r)$ satisfies 1 as $g(5) = 5$, $g(1) = 1$ and $-vr < g(r) < vr$ for all $r \in (1,5)$. The resulting trajectory is annular as shown in Fig. 1. Using (13), control law is given by $f(r) = 0.75(r-3)$. Initial conditions are chosen as $r_0 = 5$ and $\phi_0 = 3\pi/2$.

TABLE I: Simulation and Experimental results

Type of Switching	$g_1(r)$	$g_2(r)$	$g_i(r)$	R_{max_1}	R_{min_1}	R_{max_2}	R_{min_2}	Switching Points
Direct	$\frac{r^3}{520}+\frac{2400}{13}$	$\frac{r^3}{1560}+\frac{56000}{156}$	NA	Simulated: 60 Experiment: 61.31	Simulated: 20 Experiment: 18.17	Simulated: 100 Experiment: 101.6	Simulated: 40 Experiment: 37.63	$\bar{r}=51.43$
	$\frac{6r^3}{5600}-\frac{200}{7}$	$-3r+80$	NA	Simulated: 40	Simulated: 20	Simulated: 40	Simulated: 20	$\bar{r}=28.19$
Indirect	$0.2r^2-2r$	$0.2r^2-6r$	$\frac{8r^3}{1000}-\frac{32r^2}{100}+2.4r$	Simulated: 15	Simulated: 5	Simulated: 35	Simulated: 25	$\bar{r}_1=10$ $\bar{r}_2=30$
	$\frac{r^3}{390}+\frac{7000}{39}$	$\frac{r^3}{2190}+\frac{11900}{219}$	$\frac{r^3}{970}+\frac{26400}{97}$	Simulated: 50 Experiment: 51.32	Simulated: 20 Experiment: 18.88	Simulated: 100 Experiment: 102.4	Simulated: 70 Experiment: 67.02	$\bar{r}_1=39.25$ $\bar{r}_2=77.87$

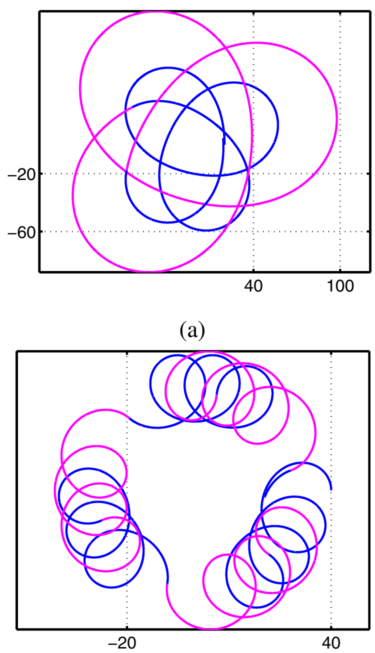

(a)

(b)

Fig. 4: Direct Switching

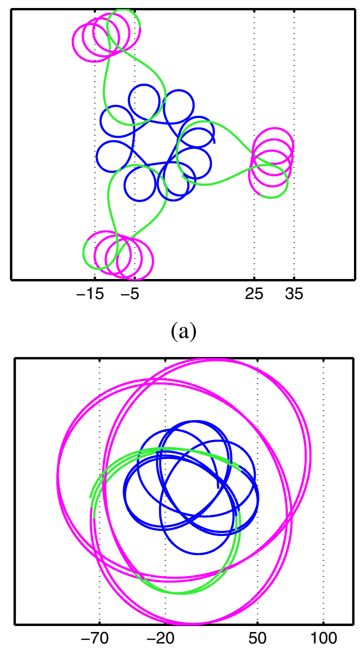

(a)

(b)

Fig. 5: Indirect Switching

Case 2 - *Direct Switching*: Here, the bounds of the patterns among which trajectory is switched are: $R_{\max 1}$, $R_{\min 1}$, $R_{\max 2}$ and $R_{\min 2}$. It can be verified that corresponding generating functions satisfy conditions given in Lemma 2. Then, the agent generates the desired switching trajectory. Table I gives some feasible generating functions to validate the direct switching strategy and the corresponding agent trajectories are shown in Fig. 4.

Case 3 - *Indirect Switching*: The bounds of the patterns among is switching is desired are given as $R_{\max 1}$, $R_{\min 1}$, $R_{\max 2}$ and $R_{\min 2}$. An intermediate generating function is designed using Theorem 1. Then, the agent generates the desired switching trajectory. Two cases are given to demonstrate indirect switching law with trajectory plots shown in Fig. 5 and the other details given in Table. I

V. Hardware Setup and Experimental Results

For the experimental results presented, the Firebird V differential drive robot has been used as a testbed to validate the direct switching and indirect switching strategies. The Firebird V robot is equipped with motors having an angular speed range of 2.7 rad/s to 6.67 rad/s which corresponds to a linear speed range of 7 cm/s to 17 cm/s. The robot is also fitted with a XBee® Pro Series 1 trans-receiver module, and a black and white visual pattern on a mount board as shown in Fig. 7. A visual feedback system, developed in house, measures the pose of the robot from the visual pattern using a calibrated camera. This information of robot position (x_r, y_r) and heading α_r with time stamp is communicated to the robot every 0.15 sec via a serial communication link using Xbee modules. The differential drive robot is modeled with unicycle kinematics, i.e., $\dot{x}_r(t) = V_r(t)\cos(\alpha_r(t))$, $\dot{y}_r = V_r(t)\sin(\alpha_r(t))$ and $\dot{\alpha}_r = \omega_r(t)$, where the inputs to the system $V_r(t)$ and $\omega_r(t)$ are the linear and angular velocities of the robot at instantaneous position $P_r(t) = (x_r(t), y_r(t))$ and heading $\alpha_r(t)$. The robot's initial position and heading are approximately equal to the initial position $P_L = (x_L, y_L)$ and orientation α_L of the reference point on the desired curve. The motion of reference point is then propagated by the robot using a Runge-Kutta fourth order solver and

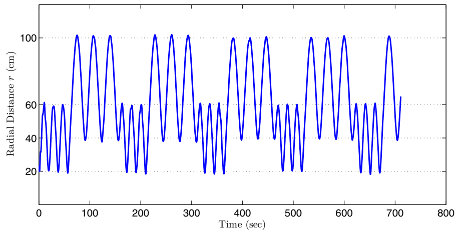

(a) Direct Switching

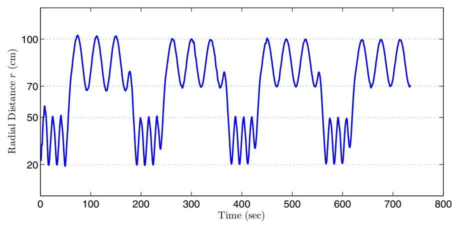

(b) Indirect Switching

Fig. 6: $r \sim t$ plots

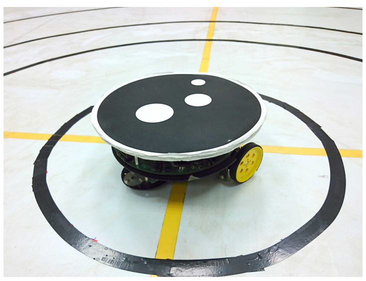

Fig. 7: Firebird V robot with a black and white pattern for visual pose detection and feedback

the heading rate of the reference point is given by $\dot{\alpha}_L(t) = f(r) = \frac{1}{r}\frac{d}{dr}g(r)$ where r is the distance of the reference point from the origin and $g(r)$ is the generating function. The robot computes a heading towards the reference point as $\alpha_c = \arctan\left(\frac{y_L(t)-y_r(t)}{x_L(t)-x_r(t)}\right)$. Using the reference point heading rate $\dot{\alpha}_L(t)$ and the heading error $e_\alpha = \alpha_c - \alpha_r$, the robot velocities $V_r(t)$ and $\omega_r(t)$ are commanded as follows:

$$V_r(t) = K_v \cos(e_\alpha) D_r, \;\; \omega_r(t) = K_\alpha e_\alpha + \dot{\alpha}(t) \qquad (18)$$

where K_v and K_α are controller gains and D_r is the Euclidean distance between the robot the reference point. In [14], the authors show that, using this control law, the agent remains within a bounded distance of the reference point while moving on a smooth trajectory. $V_r(t)$ and $\omega_r(t)$ are then translated to motor speed commands using the equations relating the unicycle model and differential drive robot given in [15].

The experiments have been performed for the both direct and indirect switching. The data of the experiments have been compared with the simulation for the same case in Table I. The video link for the direct and indirect switching experiments are http://www.sc.iitb.ac.in/∼asinha/videos/patterns/directswitching.mp4 and http://www.sc.iitb.ac.in/∼asinha/videos/patterns/indirectswitching.mp4. For all the experimental results presented, the control gains used are $K_v = 1.5$, $K_\alpha = 1.1$, and the velocity of the reference point on the curve is assumed to be $V_L = 11$ cm/s. The variation of r with time is shown in Fig. 6.

VI. Conclusion

The paper presents a control law to generate bounded patterns in a plane using a single autonomous agent, modelled as a unicycle. Assuming the availability of only range information, the control law is designed as any continuous function of range to generate patterns. Necessary conditions are given under which the agent trajectory is guaranteed to trace bounded (annular) and periodic patterns using this control law. Further, a switching strategy is proposed to switch the agent trajectory between any two desired annular periodic patterns. The theoretical results have been illustrated through simulations. Hardware experiments have also been performed to demonstrate the various cases under the switching strategy. The proposed results can also be extended for multi-agent systems.

References

[1] K. -K. Oh, M. -C. Park, and H. -S . Ahn,“A survey of multi-agent formation control,” Automatica, Vol. 53, no. 3, pp. 424-440, 2015.

[2] M. Mischiati and P. S. Krishnaprasad, “The dynamics of mutual motion camouflage,” *Systems & Control Letters*, vol. 61, pp. 894-903, 2012.

[3] A. Morro, A. Sgorbissa, and R. Zaccaria, “Path following for unicycle robots with an arbitrary path curvature,” *IEEE Transactions on Robotics*, vol. 27, no. 5, pp. 1016-1023, 2011.

[4] J. -C. Juang, “On the formation patterns under generalized cyclic pursuit,” *IEEE Transactions on Automatic Control*, vol. 58, no. 9, pp. 2401-2405, 2013.

[5] K. S. Galloway, E. W. Justh and P. S. Krishnaprasad, “Portraits of cyclic pursuit,” *Proc. of the 42nd IEEE Conference on Decision and Control*, pp. 2724-2731, Orlando, Florida, Dec. 2011.

[6] K. S. Galloway, E. W. Justh and P. S. Krishnaprasad, “Symmetry and reduction in collectives: cyclic pursuit strategies,” *Proc. of The Royal Society*, http://dx.doi.org/10.1098/rspa.2013.0264.

[7] P. Tsiotras and L. I. R. Castro, “Extended multi-agent consensus protocols for the generation of geometric patterns in the plane,” *Proc. of the American Control Conference*, pp. 3850-3855, San Francisco, USA, June 2011.

[8] P. Tsiotras and L. I. Reyes Castro, “The Artistic Geometry of Consensus Protocols,” in *Controls and Art*, Springer International Publishing, pp. 129-153, 2014.

[9] T. Tripathy and A. Sinha, “Guidance of an autonomous agent for coverage applications using range only measurement,” *Proc. of AIAA, Guidance, Navigation & Control Conf.*, Boston, USA, August 2013, http:dx.doi.org/10.2514/6.2013-5095.

[10] T. Tripathy and A. Sinha, “A guidance law for a mobile robot for coverage applications: A limited information approach,” *Third Int. Conf. on Advances in Control and Optimization of Dyn. Systems*, pp. 437-442, Kanpur, India, March 2014.

[11] T. Tripathy and A. Sinha “A Control Scheme to Achieve Coverage Using Unicycles,” *Indian Control Conference*, pp. 494-499, Chennai, India, January, 2015.

[12] T. Tripathy and A. Sinha “Generating Patterns Using Unicycles,” *Transactions on Automatic Control*, DOI 10.1109/TAC.2015.2503891.

[13] G. F. Simmons, *Differential Equations with Applications and Historical Notes*, 2^{nd} edition, New York:McGraw-Hill, 2003.

[14] G. M. Atinc, D. M. Stipanovic, P. G. Voulgaris and M. Karkoub, “Collision-free trajectory tracking while preserving connectivity in unicycle multi-agent systems,” *In Proc. of American Control Conference*, pp. 5392-5397, Washington DC, USA, June 2013.

[15] S. G. Tzafestas, *Introduction to mobile robot control*, 1^{st} edition, Elsevier Science Publishing Co Inc., 2013.